ECCD Experiment Using an Upgraded ECH System on LHD

ECCD Experiment Using an Upgraded ECH System on LHD*)

Yasuo YOSHIMURA, Shin KUBO, Takashi SHIMOZUMA, Hiroe IGAMI, Hiromi TAKAHASHI, Masaki NISHIURA, Shinya OGASAWARA[1)], Ryohei MAKINO[1)], Katsumi IDA, Mikiro YOSHINUMA, Satoru SAKAKIBARA, Kenji TANAKA, Kazumichi NARIHARA, Takashi MUTOH, Hiroshi YAMADA, Kazunobu NAGASAKI[2)], Nikolai B. MARUSHCHENKO[3)] and Yuri TURKIN[3)]

National Institute for Fusion Science, Toki 509-5292, Japan
[1)]*Department of Energy and Technology, Nagoya University, Nagoya 464-8463, Japan*
[2)]*Institute of Advanced Energy, Kyoto University, Uji 611-0011, Japan*
[3)]*Max-Planck-Institut for Plasmaphysik, IPP-EURATOM Association, D-17491 Greifswald, Germany*

(Received 9 December 2011 / Accepted 13 February 2012)

Electron cyclotron current drive (ECCD) is an attractive tool for controlling plasmas. In the large helical device (LHD), ECCD experiments have been performed by using an EC-wave power source, gyrotron, with a frequency of 84 GHz. The maximum driven current was ~9 kA with 100 kW injection power to plasma and 8 s duration of EC-wave pulse. These years, high-power and long-pulse 77 GHz gyrotrons were newly installed. An ECCD experiment with 775 kW injection power was performed. The 77 GHz waves of 8 s pulse duration sustained the plasmas. The EC-wave beam direction was scanned toroidally, keeping the beam direction aiming at the magnetic axis in X-mode polarization. In spite of the change in the EC-wave beam direction, plasma parameters such as the line-average electron density, the central electron temperature and the plasma stored energy were kept nearly the same values for the discharges, $\sim 0.3 \times 10^{19}\,\mathrm{m}^{-3}$, ~3 keV and ~30 kJ, except for the plasma current. The plasma current showed a systematic change with the change in the beam direction for ECCD, and at an optimum direction with $N_{//} \sim -0.3$, the plasma current reached its maximum, ~40 kA. Also, current drive efficiency normalized with density and power was improved by 50% compared with that at the former 84 GHz ECCD experiment.

Keywords: electron cyclotron current drive, ECCD, plasma current, gyrotron, LHD, TRAVIS

DOI: 10.1585/pfr.7.2402020

1. Introduction

Electron cyclotron current drive (ECCD) is an attractive tool for controlling plasmas. By using a well-focused EC-wave beam, the plasma current can be driven locally so that ECCD can control the plasma current and rotational transform profiles, which affect magnetohydrodynamics (MHD) activity [1–3]. In tokamak-type plasma confinement devices, the effectiveness of ECCD for stabilizing the neoclassical tearing mode, which is a harmful MHD activity, has been demonstrated by driving current within the magnetic island [4–7]. Moreover, ECCD can be suitable for assisting ohmic plasma current startup in tokamaks.

Also, for stellarators that do not need plasma current for plasma confinement, the current profile control capability enables fine plasma control. ECCD can maintain an optimized profile of the rotational transform $\iota/2\pi$ or locally modify the $\iota/2\pi$ profile if it is needed. Elimination or shifting of the rational surfaces suppresses instabilities related to the existence of the surfaces. In the Wendelstein 7-AS stellarator [8] and helical systems: Heliotron J [9–11] and compact helical system (CHS) [12, 13], well-constructed ECCD experiments were conducted and the results were investigated in detail. Also in large helical device (LHD), ECCD experiments have been performed by use of an 84 GHz ECH/ECCD system. Basic characteristics of ECCD such as dependence of EC-driven current on the EC-wave beam direction were investigated [14, 15].

These years, upgrade of ECH/ECCD system on LHD by introducing high-power, long-pulse 77 GHz gyrotrons made a successful progress [16]. One of the three new 77 GHz gyrotrons was connected to an ECCD-applicable injection antenna system with a transmission line.

This paper describes the results of recent ECCD experiments using the upgraded ECH/ECCD system in LHD. The LHD and the system for the ECCD experiment are briefly described in Sec. 2. Section 3 describes results of ECCD experiments that show significant improvements in EC-driven current and current drive efficiency. Then the contents of this paper are summarized in Sec. 4.

author's e-mail: yoshimu@ms.nifs.ac.jp
*) This article is based on the presentation at the 21st International Toki Conference (ITC21).

2. LHD and ECCD System

LHD is a helical device with a toroidal period number $m = 10$ and a polarity $l = 2$. A magnetic field structure with a rotational transform for plasma confinement is generated entirely by external superconducting coils such as two helical coils and three pairs of poloidal coils [17]. The major radius, or the position of the magnetic axis R_{ax} of the LHD plasma, can be varied in the range of 3.42-4.1 m. The average plasma minor radius is ~0.6 m, and the maximum magnetic field at the magnetic axis is ~3 T. These values and the characteristics of the magnetic field structure, such as rotational transform profile and magnetic field along the magnetic axis, vary depending on R_{ax}.

The magnetic field distribution along the magnetic axis in the magnetic field configuration with $R_{ax} = 3.75$ m is nearly constant and the magnetic ripple is only 0.14% whereas with $R_{ax} = 3.6$ or 3.9 m, the magnetic ripples up to ~5% exist [15]. The ECCD experiments described in this study were performed with the magnetic field configuration of $R_{ax} = 3.75$ m to minimize the effect of magnetic ripples, that is, mirror-trapping effect on ECCD.

The EC-wave beam injection system that is applicable for ECCD experiment has to furnish a two-dimensionally and widely steerable mirror that enables beam direction control. The beam injection system consists of two inner-vessel mirrors. One of the mirrors transforms the EC wave beam shape, which is radiated from a waveguide for EC-wave transmission, to a focused Gaussian beam. The other plane mirror is used to change the beam direction.

Previous ECCD experiments were performed using an 84 GHz gyrotron with a capability of long-pulse operation, though the output power was limited rather low up to 160 kW, and the beam injection system was installed at the bottom port of the LHD (1.5-L port) [14, 15].

These years, an upgrade of ECH system on LHD is ongoing. High-power, long-pulse 77 GHz gyrotrons were newly installed. The output powers for several seconds and for continuous operation are over 1.0 MW and 0.3 MW, respectively. A beam injection system at a horizontal port (2-O port) used for one of the 77 GHz gyrotrons furnishes widely tiltable plane mirror so that the 77 GHz ECH system can be used for ECCD experiments with high power and long pulse. The ECCD experiments described in this paper were performed with the magnetic field on the magnetic axis of 1.375 T, which is the second harmonic resonance field for the frequency of 77 GHz.

The EC-wave beams are injected from the low magnetic field side (LFS) in both the beam injection configurations of 84 GHz and 77 GHz systems.

3. Achievement of Large EC-Driven Current with Upgraded ECCD System

The EC-wave beam direction should be toroidally tilted for ECCD. Figure 1 shows a schematic representation that illustrates the experimental configuration, EC-wave beam direction $N_{//}$, and plasma current direction. $N_{//}$ is defined as the cosine of the angle between the beam unit vector and the tangent of the magnetic axis at the cross point of the beam and the magnetic axis. For the help of understanding, an example of EC-wave beam projected on a poloidal cross section is plotted in Fig. 2. According to the Fisch-Boozer theory [18], an EC-wave beam injected from the LFS with positive (negative) $N_{//}$ couples primarily with electrons moving in the negative (positive) I_p direction, thus the wave is expected to generate an EC-driven current in the positive (negative) I_p direction.

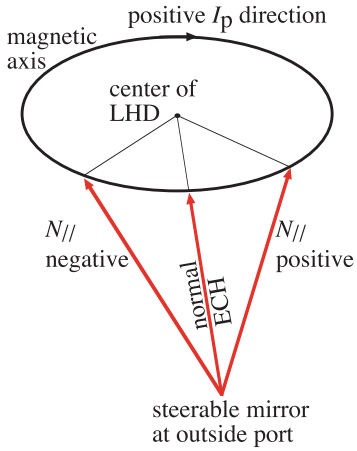

Fig. 1 Schematic view of ECCD experimental configuration. EC-wave beams are obliquely injected in toroidal direction from an outside port, aiming at the magnetic axis.

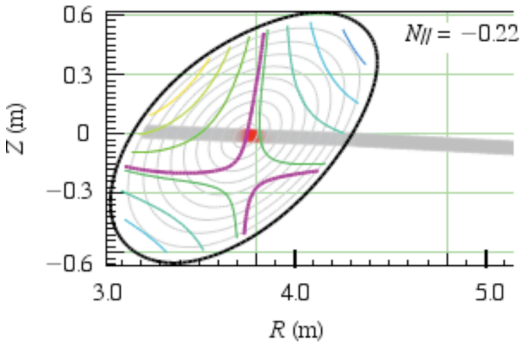

Fig. 2 An example of EC-wave beam (in gray) projected on a poloidal cross section in an ECCD configuration. Hyperbolic-like curves in pink denote 2nd harmonic resonance layers. Concentric ellipses are flux surfaces.

A set of discharge waveforms in the ECCD experiment is plotted in Fig. 3. The plasma was generated at 1 s with 300 ms pulses of 82.7 and 84 GHz waves, and a 77 GHz wave of 775 kW injection power sustained the plasma for 8 s. The 77 GHz wave was obliquely injected and aimed at the magnetic axis with $N_{//}$ of −0.29 and with right-hand circular polarization, which is close to the X mode in the case of oblique injection.

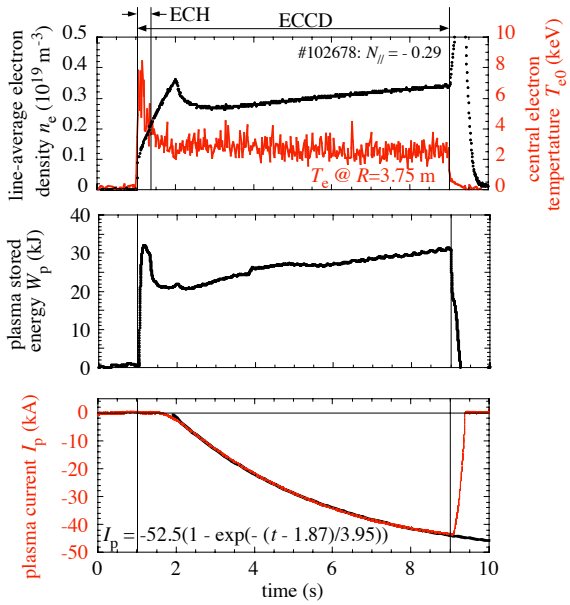

Fig. 3 Waveforms in an ECCD discharge. Top: line-average electron density (black) and central electron temperature (red), middle: plasma stored energy and bottom: plasma current (red) and its fitting curve (black).

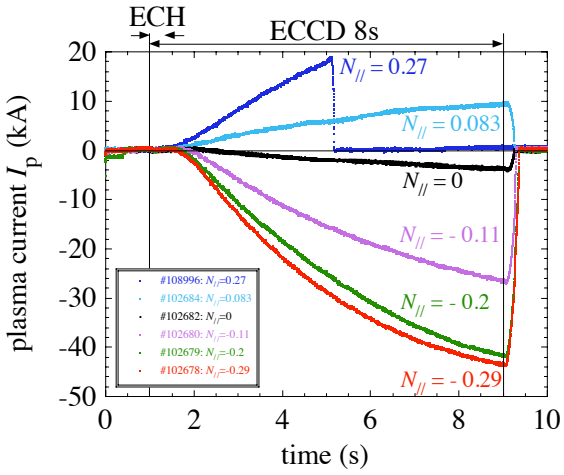

Fig. 4 Time evolutions of plasma current in the discharges with various EC-wave beam direction.

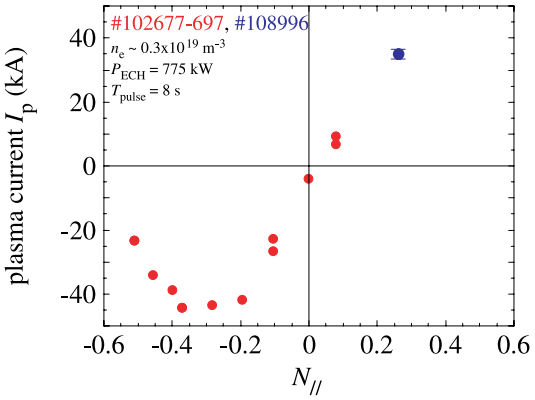

Fig. 5 Dependence of plasma current I_p at the end of the discharges (at 9 s) is plotted as a function of EC-wave beam direction $N_{//}$. The data point with $N_{//} = 0.27$ is an extrapolation from the discharge with 4 s duration.

Except for the transitional initial 1.5 s period, the line-average electron density n_e, the electron temperature T_{e0} at the magnetic axis (R = 3.75 m, measured with Thomson scattering system) and the plasma stored energy W_p do not vary so much and are kept nearly constant at 0.3×10^{19} m^{-3}, 2.7 keV and 28 kJ for 6.5 s until the end of the discharge. On the contrary, the plasma current I_p (plotted in red) is kept increasing during the discharge. An exponentially saturating fitting curve is also plotted (in black) with the time evolution of I_p. For the fitting, I_p data in the range from 2 s to 9 s were used. According to the fitting, the time constant of the current saturation and the saturated current are evaluated to be 3.95 s and −52.5 kA, respectively. With other $N_{//}$ values, the time constant scatters in the range of about 4~8 s. Thus, to confirm the saturated current precisely, even longer pulse width is required. However, from the limitations of data acquisition and gyrotron operation, the pulse width was set as 8 s and the driven current was evaluated at the end of EC-wave injection (here it was −43.6 kA at 9 s).

In a scan of EC-wave beam direction, $N_{//}$, the beam direction was toroidally scanned while maintaining the beam's aiming position on the magnetic axis. The wave polarization was right-hand circular for non-zero $N_{//}$. The electron density was kept at 0.3×10^{19} m^{-3}. The electron temperature had peaked profile and the central electron temperature was ~3 keV. Time evolutions of plasma current I_p with various $N_{//}$ values are plotted in Fig. 4. EC-wave pulse width was 8 s except for the discharge with $N_{//}$ of 0.27 (pulse width was set as 4 s).

$N_{//}$ was scanned in the range of −0.51~0.27, as summarized in Fig. 5 where I_p at the end of the discharges (9 s) is plotted as a function of $N_{//}$. At negative $N_{//}$, I_p negatively increases with $N_{//}$ until $N_{//}$ reaches ~ −0.3 and then it decreases with $N_{//}$. Main reason of the I_p degradation at large $|N_{//}|$ is considered as an increase in absorbed EC-wave power to electrons trapped in the magnetic ripples at off-axis region with too large $N_{//}$ [15]. To avoid interference of EC-wave beam with the edge of LHD vacuum vessel, maximum positive $N_{//}$ should be limited smaller than 0.27.

Extrapolation of the I_p value with $N_{//} = 0.27$ to that at 9 s tells that I_p with $N_{//} = 0.27$ at 9 s should be 35 ± 1.5 kA. Assuming that the bootstrap current does not vary with $N_{//}$ and is equal to I_p with $N_{//} = 0$, ~ −4 kA, large EC-driven current of ~40 kA flowing both the positive and negative directions are successfully generated with the upgraded 77 GHz ECCD system in LHD, while the maximum EC-driven current obtained with the former 84 GHz ECCD system was 9 kA, with the injection power of 100 kW, the

line-average electron density of $0.1 \times 10^{19}\,\mathrm{m}^{-3}$ and the central electron temperature of ~3 keV.

The current drive efficiencies γ_{77} with the upgraded ECCD system and γ_{84} with former one, defined as $\gamma = n_e R_{ax} I_{ECCD}/P_{abs}$ are compared. γ_{84} is evaluated as $3.9 \times 10^{17}\,\mathrm{AW}^{-1}\,\mathrm{m}^{-2}$ [15]. Here, absorbed power P_{abs} was estimated as 87 kW from a calculation by TRAVIS code [19] applied to LHD. γ_{77} is evaluated as $5.8 \times 10^{17}\,\mathrm{AW}^{-1}\,\mathrm{m}^{-2}$ (P_{abs} = 774 kW from TRAVIS) so that γ_{77} is 1.5 times larger than γ_{84}. So the upgraded system is more favorable for ECCD than expected from the effect of power-up. According to the TRAVIS calculation, a part of this improvement in γ is attributed to a reduction of power absorption by the electrons trapped in magnetic ripples at off-axis region, due to the difference in the heating configurations.

4. Conclusions

Results of ECCD experiment performed with upgraded 77 GHz ECH/ECCD system on LHD was described. Applying higher EC-wave injection power of 775 kW for 8 s, significant EC-driven currents up to 40 kA were generated in both the negative and positive directions, in accordance with the change in the EC-wave beam direction. The electron density was $\sim 0.3 \times 10^{19}\,\mathrm{m}^{-3}$ in the discharges. The maximum driven current in the former 84 GHz ECCD experiment was ~9 kA with 100 kW injection power for the density of $0.1 \times 10^{19}\,\mathrm{m}^{-3}$. Thus, by the upgraded high-power 77 GHz ECH/ECCD system, not only the magnitude of EC-driven current but also current drive efficiency normalized with the power and the electron density are much improved.

The powerful ECCD will contribute to improvements in LHD plasma performance through the control of plasma current and rotational transform profiles, and stabilization of MHD activities.

Acknowledgments

The authors thank the NIFS staff for performing the LHD experiments. This work was conducted under the framework of a bidirectional collaborative research program between Kyoto University and the National Institute for Fusion Science (KOAR010, KLRR304). This work was partly supported by KAKENHI (Grant-in-Aid for Scientific Research (C), 21560862).

[1] V. Erckmann and U. Gasparino, Plasma Phys. Control. Fusion **36**, 1869 (1994).
[2] B. Lloyd, Plasma Phys. Control. Fusion **40**, A119 (1998).
[3] R. Prater, Phys. Plasmas **11**, 2349 (2004).
[4] H. Zohm *et al*., Nucl. Fusion **39**, 577 (1999).
[5] R. Prater *et al*., Nucl. Fusion **47**, 371 (2007).
[6] A.C.C. Sips *et al*., Nucl. Fusion **47**, 1485 (2007).
[7] A. Isayama *et al*., Nucl. Fusion **49**, 055006 (2009).
[8] H. Maassberg *et al*., Plasma Phys. Control. Fusion **47**, 1137 (2005).
[9] G. Motojima *et al*., Nucl. Fusion **47**, 1045 (2007).
[10] K. Nagasaki *et al*., Nucl. Fusion **50**, 025003 (2010).
[11] K. Nagasaki *et al*., Nucl. Fusion **51**, 388704 (2011).
[12] Y. Yoshimura *et al*., J. Korean Phys. Society **49**, S197 (2006).
[13] Y. Yoshimura *et al*., Fusion Sci. Technol. **53**, 54 (2008).
[14] Y. Yoshimura *et al*., Fusion Sci. Technol. **58**, 551 (2010).
[15] Y. Yoshimura *et al*., J. Plasma Fusion Res. **6**, 2402073 (2011).
[16] H. Takahashi *et al*., Fusion Sci. Technol. **57**, 19 (2010).
[17] A. Komori *et al*., Fusion Sci. Technol. **58**, 1 (2010).
[18] N.J. Fisch and A.H. Boozer, Phys. Rev. Lett. **45**, 720 (1980).
[19] N.B. Marushchenko *et al*., Phys. Plasmas **18**, 032501 (2011).